Almost sudden perturbation of a quantum system with ultrashort electric pulses

Andrey Lugovskoy* and Igor Bray
Department of Imaging and Applied Physics, Curtin University, Perth 6150, Australia
(Received 23 October 2007; revised manuscript received 13 December 2007; published 29 February 2008)

We present an alternative approach to analyze atomic behavior when an external field perturbation is not sudden for a number of states of the field-free system. It is shown that the probability amplitudes for the system to be in these states can be accurately estimated from the closed set of their integral equations. Numerical examples for an electron in a one-dimensional Coulomb potential interacting with (i) laser and (ii) half-cycle pulses are provided. Comparison with exact calculations indicates the strength of the approach.

DOI: 10.1103/PhysRevA.77.023420 PACS number(s): 42.50.Hz, 32.90.+a, 32.80.Rm

I. INTRODUCTION

In many physical processes of practical importance compound quantum systems undergo pulsed perturbations. For example, such situations occur when atomic particles are subjected to external pulsed fields [1] or collide with each other [2]. Generally, the time evolution of perturbed systems cannot be derived analytically from first principles and numerical solution is needed. This is often exceptionally challenging, consuming considerable computer time and memory [1,3], and often impossible without approximations.

Approximate solutions can be indispensable in guiding costly numerical methods. To use approximations we need criteria to separate important aspects of the problem from those which can be neglected. If either the applied field magnitude or the characteristic field magnitude in the initial system is small with respect to the other the solution can be expressed as a perturbation series [4,5]. Generally, no restriction on the interaction time is required within such an approach.

The sudden perturbation approximation (SPA) was developed specifically for time-dependent processes of very short duration, satisfying the inequality

$$\kappa = |\epsilon|\tau \ll 1, \tag{1}$$

where τ is the time of perturbation (we also call it the interaction time) and ϵ is the eigenenergy of any of the essential states. These are the unperturbed states populated with sufficiently high probability during the interaction. We use atomic units in Eq. (1) and throughout unless specified otherwise.

If condition (1) is met the perturbation is so sudden that the system literally has no time to respond. Its evolution during the interaction is mainly driven by the time-dependent perturbation potential $\hat{V}$. The contribution of the unperturbed Hamiltonian $\hat{H}_0$ is of the first order of κ and can be neglected. One can do better by expanding the evolution operator $\hat{S}(t,t_0)$ in a series over small parameter κ. It leads to the expression [6]

$$\hat{S}(t,t_0) = \hat{S}_0(t,t_0)\left[\hat{I} + \sum_{n=1}^{\infty} \hat{\Delta}_n(t,t_0)\right], \tag{2}$$

where $\hat{I}$ is the identity operator and

$$\hat{S}_0(t,t_0) = \exp\left[-i\int_{t_0}^{t} \hat{V}(t')dt'\right] \tag{3}$$

is the zeroth order approximation. The correction terms $\hat{\Delta}_n$ in Eq. (2) depend on $\hat{H}_0$. The contribution of $\hat{\Delta}_n$ to the $\hat{S}$ operator is of the nth order in κ. The potential $\hat{V}$ is assumed to be nonzero near $t=0$. Also, this operator has to commute with itself at different instants of time. Truncating the series (2) one gets the sudden-perturbation approximation of the $\hat{S}$ operator to the nth order.

The SPA imposes no explicit restrictions on the field magnitude. So, it works well in both perturbative and nonperturbative regimes provided that no states violating inequality (1) are excited. Calculations are simple and interpretations are straightforward. For example, in the case of one active electron, Eq. (3) yields

$$\hat{S}_0(\infty,-\infty) = \exp[i\boldsymbol{p}\cdot\boldsymbol{r}], \tag{4}$$

where $\boldsymbol{r}$ is the electron position and $\boldsymbol{p} = -\int_{-\infty}^{\infty}\boldsymbol{E}(t)dt$ is the total drift momentum due to the applied field $\boldsymbol{E}$. Expression (4) is used to model the behavior of highly excited atoms whose electrons are "kicked" by half-cycle pulses [7–10].

For Rydberg atoms the zeroth approximation can be used since all essential states satisfy requirement (1). In particular, neither the ground state nor the low-lying excited states are involved. This is equally applicable to states with positive energies whenever $\epsilon \gtrsim 1/\tau$. Thus, Eq. (1) severely limits the kind of systems that may be treated with the SPA.

Here we present an approach that does away with the requirement that Eq. (1) is satisfied, while maintaining some of the strengths of the SPA. We consider the more general situation where the perturbation is not sudden for some essential states. We need to take them exactly into consideration and ensure their proper "communication" with the states satisfying condition (1).

*A.Lugovskoy@curtin.edu.au

 ©2008 The American Physical Society

The formal approach based on this idea is developed in Sec. II. In what follows we will call it the almost-sudden-perturbation approximation (ASPA). It is tested in Sec. III for the numerically solvable model. The outcomes are given in a summary.

II. THEORY

In this section we introduce an alternative approach for the description of a quantum system under the action of a pulsed perturbation. The interaction time is not supposed to be short for all states involved in the process. These states are eigenstates of the time-independent Hamiltonian $\hat{H}_0$.

Let the pulse arrive at $t=0$ and its action is complete at $t=\tau$. We want to know how the system state $|\psi(t)\rangle$ evolves from $|\psi_0\rangle$ at $t=0$ and what the final state $|\psi(\tau)\rangle$ is. In this paper we are looking for a nonrelativistic answer to our question. It can be obtained from the Schrödinger equation

$$i\frac{\partial}{\partial t}|\psi(t)\rangle = [\hat{H}_0 + \hat{V}(t)]|\psi(t)\rangle \tag{5}$$

with the initial condition $|\psi(t=0)\rangle = |\psi_0\rangle$.

The solution of Eq. (5) can be written as an expansion

$$|\psi(t)\rangle = \sum \int_n a_n(t)|\phi_n\rangle e^{-i\epsilon_n t} \tag{6}$$

in a complete set $\mathbb{S}=\{|\phi_n\rangle\}$ of the unperturbed states indexed with the list n of quantum numbers. The energy ϵ_n is an eigenenergy of $\hat{H}_0$ corresponding to the eigenstate $|\phi_n\rangle$.

To tackle the problem we employ the approach similar to that of Ref. [11], where the Hilbert space is separated into two orthogonal subspaces. We divide $\mathbb{S}$ into two subsets $\mathbb{S}_1$ and $\mathbb{S}_2$ with the use of criterion

$$\kappa_n = |\epsilon_n|\tau < \alpha \leq 1, \tag{7}$$

where α is some number which can be specified later. This condition, rather than inequality (1), gives us more flexibility in calculations. Let the set $\mathbb{S}_1$ contain all states with energies satisfying inequality (7). The perturbation appears to be sudden to all these states. The second set $\mathbb{S}_2$ is defined as $\mathbb{S}_2 = \mathbb{S} - \mathbb{S}_1$. The states of this subset require special consideration.

Figure 1 shows in black the spectrum of atomic hydrogen. It is positioned near $\tau=5$ a.u. The green (inner) and blue (outer) areas are specified, respectively, with conditions $|\epsilon|\tau < \alpha$ and $\alpha < |\epsilon|\tau < 1$. The states with energies in the green area belong to $\mathbb{S}_1$. The other states form $\mathbb{S}_2$. Note that both subsets contain discrete and continuum states. So, generally, $\mathbb{S}_2$ is never empty even when condition (7) is satisfied for all negative-energy states.

Now we split $|\psi\rangle$ into two components

$$|\psi\rangle = |\psi_1\rangle + |\psi_2\rangle, \tag{8}$$

where

$$|\psi_j\rangle = \sum \int_{n\in\mathbb{S}_j} a_n(t)|\phi_n\rangle e^{-i\epsilon_n t}. \tag{9}$$

Substituting Eqs. (8) and (9) in Eq. (5) one obtains

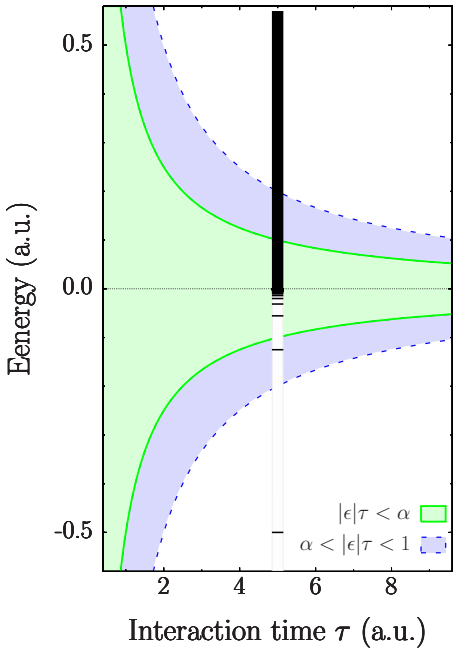

FIG. 1. (Color online) The spectrum of a hydrogen atom (black) at the background of three areas defined by the conditions $|\epsilon|\tau > 1$ (white), $\alpha < |\epsilon|\tau < 1$ (blue), and $|\epsilon|\tau < \alpha$ (green). $\alpha = 0.5$.

$$i\frac{da_m(t)}{dt} = \sum \int_{n\in\mathbb{S}_2} \langle\phi_m|\hat{W}|\phi_n\rangle a_n(t) + \langle\phi_m|\hat{W}|\chi\rangle, \tag{10}$$

$$i\frac{\partial|\chi\rangle}{\partial t} = \hat{Q}\hat{W}(t)\left(|\chi\rangle + \sum \int_{n\in\mathbb{S}_2} a_n(t)|\phi_n\rangle\right), \tag{11}$$

where $|\chi\rangle = \exp(i\hat{H}_0 t)|\psi_1\rangle$, $\hat{W}$ is the perturbation potential in the interaction representation

$$\hat{W}(t) = \exp(i\hat{H}_0 t)\hat{V}(t)\exp(-i\hat{H}_0 t), \tag{12}$$

and $\hat{Q}$ is a projection operator

$$\hat{Q} = 1 - \sum \int_{n\in\mathbb{S}_2} |\phi_n\rangle\langle\phi_n|. \tag{13}$$

In deriving Eq. (11) we took into account that $\hat{Q}$ commutes with $\hat{H}_0$. Subscript m in Eq. (10) labels the $\mathbb{S}_2$ state $|\phi_m\rangle$.

In line with the SPA one can replace $\exp(i\hat{H}_0 t)$ and $\exp(-i\hat{H}_0 t)$ in $\hat{W}$ with their Taylor series over $\epsilon\tau$ at $t=0$ when these operators act on $\mathbb{S}_1$ states. It allows one to obtain the series expansion for a_n and $|\chi\rangle$,

$$a_n = \sum_{j=0}^{\infty} a_n^{(j)}\kappa^j, \tag{14}$$

$$|\chi\rangle = \sum_{j=0}^{\infty} |\chi_j\rangle\kappa^j. \tag{15}$$

In the zero order one can derive from Eqs. (10) and (11)

$$i\frac{da_m^{(0)}(t)}{dt} = \sum \int_{n\in \mathbb{S}_2} \langle \phi_m|\hat{W}|\phi_n\rangle a_n^{(0)}(t) + \langle \phi_m|\hat{V}|\chi_0\rangle e^{i\epsilon_m t}, \tag{16}$$

$$i\frac{\partial|\chi_0\rangle}{\partial t} = \hat{Q}\hat{V}(t)\left(|\chi_0\rangle + \sum \int_{n\in \mathbb{S}_2} a_n^{(0)}(t)|\phi_n\rangle e^{-i\epsilon_n t}\right). \tag{17}$$

Equations for higher-order corrections can also be obtained which may be required if α is sufficiently close to unity.

With the use of Eq. (16) one can derive from Eq. (17)

$$|\chi_0(t)\rangle = \hat{S}_0(t,0)\hat{Q}|\psi_0\rangle - \sum \int_{n\in \mathbb{S}_2} \int_0^t dt' e^{-i\epsilon_n t'} \frac{\partial \hat{S}_0(t,t')a_n(t')}{\partial t'}|\phi_n\rangle. \tag{18}$$

Rather than substituting Eq. (18) directly in Eq. (16) to find $a_m^{(0)}$ we use the orthogonality property

$$\langle \phi_m|\chi_0(t)\rangle = 0 \tag{19}$$

for any ϕ_m from $\mathbb{S}_2$ and χ_0 being the linear combination of $\mathbb{S}_1$ functions. Substituting Eq. (18) in Eq. (19) we get

$$b_m(t) = \frac{\langle \phi_m|\hat{S}_0(t,0)|\psi_0\rangle}{\langle \phi_m|\phi_m\rangle} - i\sum \int_{n\in \mathbb{S}_2} \epsilon_n \int_0^t \frac{\langle \phi_m|\hat{S}_0(t,t')|\phi_n\rangle}{\langle \phi_m|\phi_m\rangle} b_n(t')dt', \tag{20}$$

where $b_m(t) = a_m^{(0)}(t)\exp[-i\epsilon_m t]$.

One can see that Eq. (20) for all possible m form a set of integral equations closed in respect to the probability amplitudes b_m (or $a_m^{(0)}$) only. Thus, the problem (5) is reduced to solution of the coupled set of integral Eq. (20). Once amplitudes $a_m^{(0)}$ are found $|\chi_0(t)\rangle$ can also be calculated.

Equations (18) and (20) are the main result of this paper. Their solution is an approximate solution of the Schrödinger Eq. (5) for the case when some of the states involved in the process violate the sudden-perturbation condition (7). We would like to emphasize that Eq. (20) can be derived from Eqs. (16) and (17) only if $\mathbb{S}_1$ is not empty [see, e.g., that Eq. (19) is meaningless otherwise]. As one can expect this solution converges to zero-order SPA

$$|\psi(t)\rangle \to \hat{S}_0(t,0)|\psi_0\rangle \tag{21}$$

as the interaction time τ tends to zero.

III. RESULTS AND DISCUSSION

In this section our aim is to test the approach developed in Sec. II.

A. Model system

Consider an electron in the one-dimensional soft-Coulomb potential [12–15]

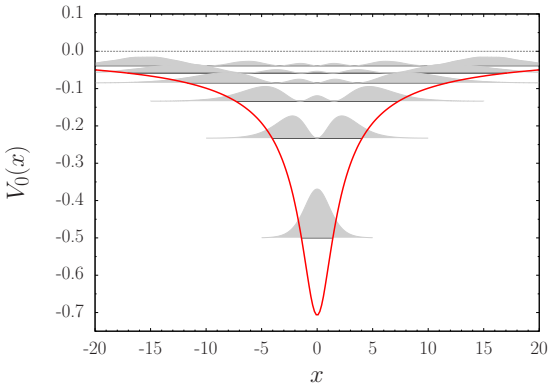

FIG. 2. (Color online) Soft Coulomb potential $\hat{V}_0$. The shaded areas show electron density distributions $|\varphi_n(x)|^2$ for several bound states. The bottom lines of these areas coincide with the energy level positions of the corresponding states.

$$\hat{V}_0(x) = -\frac{1}{\sqrt{x^2+2}}. \tag{22}$$

This potential is able to bind the electron in states with negative energies (see Fig. 2). The electron distribution densities for some of them are also shown in the figure. There is no analytical solution of the eigenstate problem with the Hamiltonian

$$\hat{H}_0 = -\frac{1}{2}\frac{d^2}{dt^2} + V_0(x). \tag{23}$$

So, we calculate eigenfunctions and eigenvalues of $\hat{H}_0$ numerically.

The apparent difficulty which can arise when solving the set (20) is accounting for the $\mathbb{S}_2$ continuum which is not taken into account in the framework of the SPA [16]. To estimate its contribution we adopt the continuum-discretization technique developed for the theory of electron-atom collisions [17]. In the framework of this approach the target electron is described with the use of pseudo state expansion. In our case it is

$$|\psi_N(t)\rangle = \sum_{n=1}^{N} b_n^N(t)|\phi_n^N\rangle, \tag{24}$$

where $b_n^N(t) = a_n^N(t)\exp[-i\epsilon_n^N t]$ are time-dependent coefficients, $|\phi_n^N\rangle$ is a nth pseudostate characterized with its pseudoenergy ϵ_n^N. The number of pseudostates N is a variable parameter.

Pseudostates are orthogonal to each other. They are obtained upon diagonalization of the Hamiltonian $\hat{H}_0$ in some truncated orthogonal basis of size N. That is, they satisfy

$$\langle \phi_m^N|\hat{H}_0|\phi_n^N\rangle = \epsilon_n^N \delta_{mn}. \tag{25}$$

Solving Eq. (25) one gets all pseudoenergies ϵ_n^N and pseudo-wave-functions

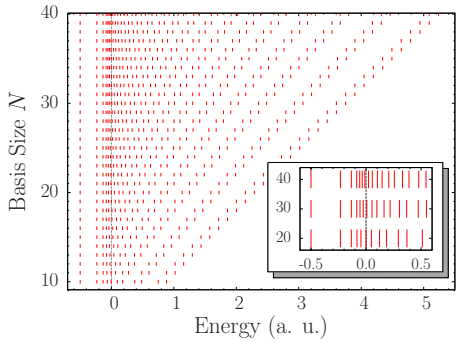

FIG. 3. (Color online) Pseudoenergy spectra for different number of basis functions N.

$$\phi_n^N(x) \equiv \langle x|\phi_n^N\rangle = \sum_{k=1}^{N} C_{nk}\xi_k(x), \tag{26}$$

where ξ_k is the kth basis function. The subscript n in ϵ_n^N and ϕ_n^N is a quantum number which we shall use to label the pseudostate. One can use different basis sets. In our case we choose the Hermite basis with

$$\xi_k(x) = \sqrt{\frac{\lambda}{\pi^{1/2}2^n n!}} H_n(\lambda x)\exp\left[-\frac{(\lambda x)^2}{2}\right], \tag{27}$$

where λ is an arbitrary parameter. Pseudostates $|\phi_n^N\rangle$ mimic true eigenstates $|\phi_n\rangle$ of same energies $\epsilon_n = \epsilon_n^N$ in the vicinity of the attractive center. This is demonstrated in Figs. 3 and 4. Figure 3 shows pseudoenergies of the Hamiltonian $\hat{H}_0$ calculated for different N. We see that the negative-energy levels converge to some constant values. Our calculations indicate that these values are equal to corresponding true eigenenergies. Positive pseudoenergies show no signs of convergence. They get more dense near zero and span a wider energy region for larger N.

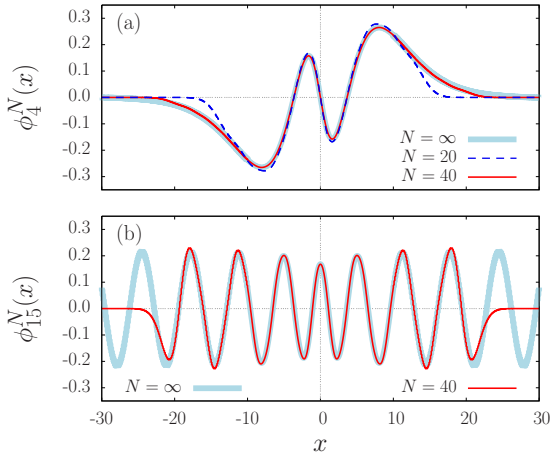

FIG. 4. (Color online) Eigenfunctions and corresponding pseudofunctions for (a) the bound state $n=4$ ($\epsilon_4 \approx -0.1$) and (b) the continuum state of energy $\epsilon \approx 0.4$. Note that $\epsilon_n = \epsilon$ at $n=15$ at $N=40$. The functions marked with $N=\infty$ are true eigenfunctions.

Figure 4 shows how pseudo-wave-functions are related to true eigenfunctions. Figure 4(a) presents the case of a localized state. The broken blue and solid red lines show pseudo-wave-functions $\phi_4^{N=20}$ and $\phi_4^{N=40}$, respectively. We compare them with the true eigenfunction ϕ_4 shown with the thick light blue line. One can see that the true eigenstate can be well reproduced when a sufficiently large basis is used.

For unbound states this can be done only for a limited range of coordinate x as demonstrated in Fig. 4(b). It shows the true eigenfunction ϕ_ϵ (thick blue line) and corresponding pseudo-wave-function $\phi_{15}^{N=40}$ (thin red line) of the states with equal energies $\epsilon = \epsilon_{14}^{N=40} \approx 0.4$. The size of the region where true eigenfunctions are well reproduced depends on the basis size N and parameter λ (in our calculations $\lambda = 0.4$ to ensure the fastest convergence rate for the ground state). All physical processes which we are able to describe with the pseudostate approach have to occur within this region.

Finally, by replacing the uncountable set of true eigenstates with a finite set of square-integrable pseudostates we come to our model system. The system evolution in the pseudostate representation is determined by the Schrödinger equation

$$i\frac{da_m^N}{dt} = \sum_{n=1}^{N} \langle \phi_m^N|\hat{W}|\phi_n^N\rangle a_m^N. \tag{28}$$

In what follows we use numerical solution of Eq. (28) for comparison with the solution of Eq. (20). One should note that the diagonalization (25) selects the sets of pseudostates which are different for different N. We will see that the physically meaningful content of expansion (24) is almost independent of N.

B. Laser pulse example

Let the system be perturbed by the field defined with its vector potential

$$A(t) = \frac{E_0}{\omega}\sin(\omega t)\left[\sin\left(\frac{\pi t}{\tau}\right)\right]^2, \tag{29}$$

where E_0, ω, and τ are, respectively, the field intensity, carrier frequency, and pulse duration. Equation (29) is a theoretical form which is widely used for the description of ultrashort laser pulses.

For realistic pulses the net momentum change Δp and displacement Δx of a free electron due to the electric field $E = -\partial A/\partial t$ have to be zero,

$$\Delta p = -\int_{-\infty}^{\infty} E(t)dt = 0, \tag{30}$$

$$\Delta x = \int_{-\infty}^{\infty} A(t)dt = 0. \tag{31}$$

Equation (30) is a general requirement. Equation (31) is always satisfied unless the laser medium is left polarized at the end of the pulse [5]. The field (29) meets condition (30) for any parameters. To satisfy Eq. (31) we put $\omega = 2\pi n_{\rm osc}/\tau$ with integer $n_{\rm osc} \geq 2$ being a number of field oscillations.

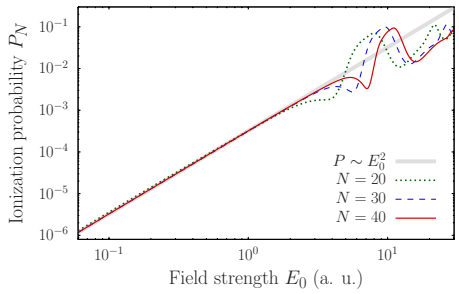

FIG. 5. (Color online) The ionization probability P_N versus the field strength E_0 calculated for three different N. The key is given in the figure. The system is initially in the ground state. The laser parameters are $\tau=5$ a.u. and $n_{\rm osc}=2$.

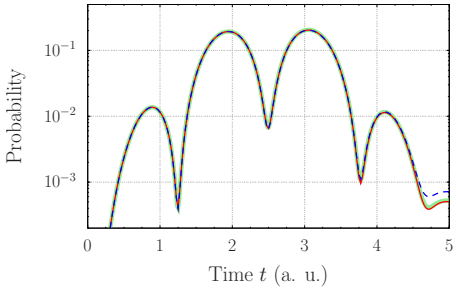

FIG. 6. (Color online) Probability $p=1-|a_1|^2$ of electron to leave initial state $n=1$ versus time. The green curve shows the exact probability p. The red and dotted-blue lines correspond to the ASPA results calculated with the different numbers of pseudostates (see text for details).

First, we would like to demonstrate that Eq. (28) yields results independent of the choice of the basis size N. To do it we calculate the ionization probabilities

$$P_N = \sum_{\epsilon_n^N>0} |a_n^N|^2 = 1 - \sum_{\epsilon_n^N<0} |a_n^N|^2 \tag{32}$$

for different N and compare them with each other. Figure 5 shows P_{20}, P_{30}, and P_{40} with the dotted green, dashed blue, and solid red curves, respectively. The pulse parameters used in the calculation were $n_{\rm osc}=2$ and $\tau=5$ a.u. The initial state is the ground state with energy $\epsilon_1=-0.5$. For this case condition (1) is violated ($\kappa_1=\epsilon_1\tau=2.5$) and the SPA is not applicable.

Figure 5 demonstrates that P_N is independent of N for $E_0<2$. For stronger fields ($E_0>2$) probabilities P_{20}, P_{30}, and P_{40} are different. Their E_0 dependences have similar resonantlike structures in this region shifted relatively to each other. We see that the larger N is, the bigger is the region where P_N can be approximated with $P\approx 3.2\times 10^{-4}E_0^2$ (gray line).

To understand this behavior we need to recall that Eq. (24) is able to approximate the true wave function if the electron stays sufficiently close to the "nucleus" during the interaction (see our discussion of Fig. 4). The electron displacement $\sim E_0$ and, hence, Eq. (24) works for relatively weak fields. A stronger field drags the electron too far where different pseudostate sets describe the process differently.

Now we are ready to solve Eq. (20) numerically and compare the results with the numerical solution of Eq. (28). Let the system be initially in the ground state. The laser parameters are the same as in the caption of Fig. 5, that is, $\tau=5$ and $n_{\rm osc}=2$. Also, to be sure that our calculations are independent of the basis set we take $E_0=1$.

Figure 6 presents the probability $p=1-|a_1(t)|^2$ for the electron to be out of the initial state during the interaction. It was obtained from the solution of Eq. (28) for $N=40$ (thick green curve). The broken-blue line shows the ASPA result calculated with the use of Eqs. (20) with $\mathbb{S}_2=\{|\phi_1^{40}\rangle,|\phi_2^{40}\rangle,|\phi_3^{40}\rangle\}$. These states violate Eq. (7) where $\alpha=0.5$.

We see that the ASPA solution is in good quantitative agreement with the reference result almost everywhere except a small interval where $t\gtrsim 4.5$. This can be anticipated if we take into account the fact that the electron quiver energy $\epsilon_{\rm osc}\approx(E_0/\omega)^2/2=0.058$ is in the energy range of the $\mathbb{S}_1$ subset defined by Eq. (7) with $\alpha=0.5$ used. Nevertheless, we see that enlargement of $\mathbb{S}_2$ with several positive-energy states with n from 10 to 16 fixes the small discrepancy (red line).

Note that the frequency ω used in this calculation is about 2.5 a.u. So, for the system being initially in the ground state, one could expect that the states with energies around $\omega-\epsilon_1\approx 2$ to be predominantly excited. However, our calculations indicate that contributions of these states are insignificant.

To understand why this is the case we show, in Fig. 7(a), how electrons are distributed over energy at the end of the pulse. The filled (red) and empty (black) circles correspond to $p_n=|a_n|^2$ calculated with the use of Eq. (28) for the states with even and odd n, respectively. Also shown with empty (blue) squares are estimations of p_n calculated with the use of the first-order perturbation theory [4]

$$p_n \approx |E(\omega_{ni})|^2|d_{ni}|^2, \tag{33}$$

where

$$E(\omega) = \int_{-\infty}^{\infty} E(t)\exp[i\omega t]dt \tag{34}$$

is the Fourier transform of the laser field strength, $\omega_{ni}=\epsilon_n-\epsilon_i$ is the transition frequency, and $d_{ni}=\langle\phi_n|x|\phi_i\rangle$ is the dipole matrix element. The latter satisfies the selection rule $d_{ni}\neq 0$ for states with odd $n+i$.

Indeed, we see from Fig. 7(a) that the energy distribution is peaked at $\epsilon=\epsilon_{16}^{40}$. Also, the exact results for the states with even n can be described reasonably well with the first-order perturbation theory. As follows from Eq. (33), the shape of the electron distribution depends on $|E(\epsilon-\epsilon_1)|^2$ and d_{n1}. These quantities are shown in Fig. 7(b). The exponentially decaying dipole matrix elements deform and shift the peak in the energy dependence of $|E(\epsilon-\epsilon_1)|^2$ from 2.5 a.u. to $\approx$0.5 a.u. Note that $E(\omega)$ is related to the Fourier image $A(\omega)$ of the vector potential $A(t)$ by $E(\omega)=\omega A(\omega)$ which results in different positions of their extrema.

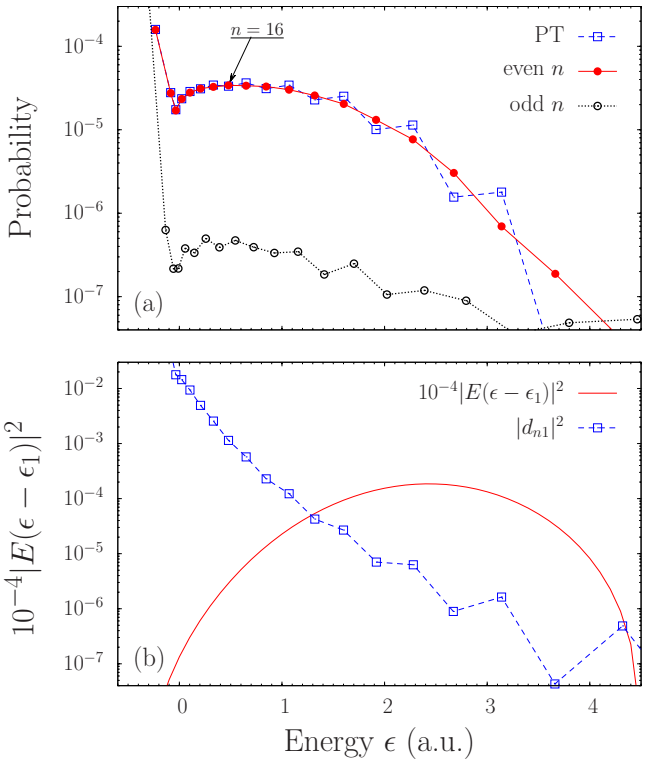

FIG. 7. (Color online) (a) Electron energy distribution at the end of the pulse. The filled red (empty black) circles correspond to probabilities $p_n=|a_n|^2$ with even (odd) n. Empty squares shows probabilities p_n calculated with the use of the perturbation theory. The lines are provided to guide the eye. (b) $|E(\epsilon-\epsilon_1)|^2$ as a function of energy ϵ (red line). Also shown with empty (blue) squares are $|d_{n1}|^2$ positioned at $\epsilon=\epsilon_n^{40}$ for all even n.

C. Half-cycle pulse example

Now we consider another example where the pulse effect on the system final state is not weak. Let the electric field be

$$E(t)=E_0\left[\frac{at^3\exp(-8t/\tau_s)}{\tau_s^3}-\frac{bt^5\exp(-t/\tau_s)}{\tau_s^5}\right], \quad (35)$$

where $a\approx 3.81\times 10^2$ and $b=4.6\times 10^{-3}$. Equation (35) is similar to the one used by [18] for a half-cycle pulse (HCP). We modify their expression to ensure that condition (30) is satisfied.

Figure 8 shows the electric field E and its vector potential A for $\tau_s=1$ a.u. The field E consists of a very short main half-cycle of duration $\sim\tau_s$. This part is followed by a long low-amplitude half-cycle pulse of opposite polarity. Usually, τ_s is considered to be small in comparison with the Kepler period T_i of an electron in the initial state $|\phi_i\rangle$. The duration of the long part τ_l is typically larger than T_i. In this case the HCP action is attributed to delivering nonzero momentum p_{HCP} to the electron by the first half cycle. The influence of the longer part on the system is usually ignored. If $\tau=\tau_s+\tau_l\ll T_i$ both parts have to be taken into account. In this case the net change in electron momentum due to the field is zero and the atom is more stable against destruction [19].

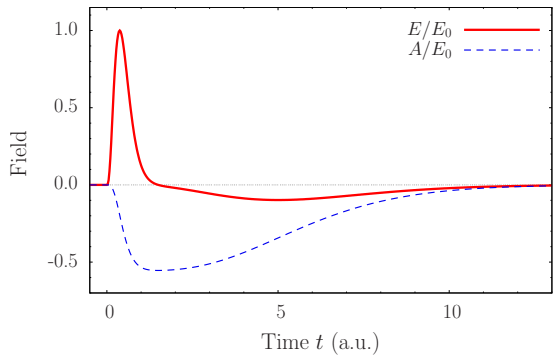

FIG. 8. (Color online) The field E of Eq. (35) and its vector potential A versus time for $\tau_s=1$.

First, we consider the case where the whole pulse duration τ is much smaller than the oscillation period T_i which is

$$T_i\approx 2\int_{-x_i}^{x_i}\frac{dx}{\sqrt{2[\epsilon_i-V(x)]}}, \quad (36)$$

where x_i is the classical turning point for the electron with energy ϵ_i in the potential (22). Equation (36) yields $T_1\approx 15.8$, $T_2\approx 43.2$, and $T_3\approx 93$ for the states with n from 1 to 3, respectively. To be sure that inequality $\tau\ll T_i$ is well satisfied we put the initial state to be $|\phi_3^N\rangle$ and $\tau_s=0.2$ a.u. The duration of the longer part τ_l is one order of magnitude larger than τ_s. So, the total pulse duration $\tau=\tau_s+\tau_l\approx 2$.

Figure 9 shows the probability $|a_3|^2$ for the system to be in the initial state during the interaction with the HCP of strength $E_0=5$. The reference result is shown with a thick light green line. The broken blue and solid red lines correspond to the ASPA results with $\mathbb{S}_2$ consisting, respectively, of three states with $n=1$ to 3 and nine states with $n=1$ to 3 and $n=8$ to 13. In Fig. 9 we also show the ionization probability P_{40} calculated with the use of Eqs. (32) and (28) (dotted brown line).

The momentum p_{HCP} received by the electron from the first half-cycle is 0.55 which corresponds to the displacement

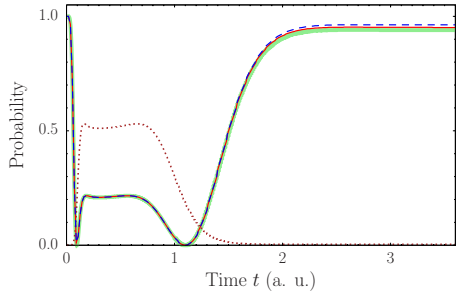

FIG. 9. (Color online) Probability $|a_3|^2$ to find the system in the initial state $n=3$ versus time. The thick light green line corresponds to $|a_3|^2$ found with Eq. (28). Two ASPA results calculated for two different sets of states (see text) are shown, respectively, with the broken blue and solid red lines. The dotted brown line corresponds to the ionization probability. The HCP parameters are $\tau_s=0.2$ ($\tau\sim 2$) and $E_0=5$.

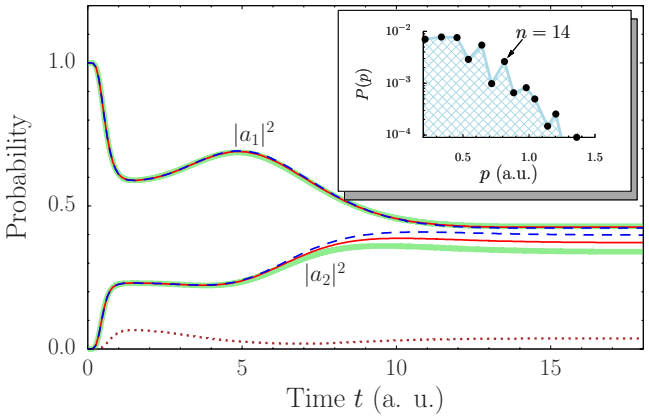

FIG. 10. (Color online) Probabilities $|a_1|^2$ and $|a_2|^2$ versus time. The initial state is $|\phi_1^{40}\rangle$. The HCP parameters are $\tau_s=1$ and $E_0=1$. Inset: $|a_n|^2$ plotted against $p_n=\sqrt{2\epsilon_n}$ at $t=18$.

$\Delta x_{\mathrm{HCP}}=p_{\mathrm{HCP}}\tau_s\approx 0.11$. Thus, the electron stays in the region where Eq. (24) is applicable during the interaction. The field E is sufficiently strong to bring the electron to the continuum. We see that it can be found there with high probability when $0.2<t<1.2$. However, when the pulse action is finished the system state is almost completely recovered, in qualitative agreement with the observations [19]. The ionization probability is very small. This behavior can be quantitatively described by the ASPA with only three negative-energy states in $\mathbb{S}_2$. A small correction is still needed. By enlarging $\mathbb{S}_2$ with several positive-energy states we get better agreement.

Let us now examine the case where τ is of the same order of magnitude as T_i. We take $\tau_s=1$ and, hence, $\tau\sim 10$. This is comparable with $T_1=15.8$. So, $|\phi_1^{40}\rangle$ is assumed to be the initial state. Figure 10 shows the probabilities $|a_1|^2$ and $|a_2|^2$. They are well separated in the figure. So we use the same line styles as those of Fig. 9. Again, the ASPA probabilities were calculated with two different sets $\mathbb{S}_2$ which include, respectively, negative-energy states only (n is from 1 to 6) (broken blue line) and both negative- and positive-energy states (n is from 1 to 6 and from 9 to 16) (solid red line).

We see that the system behaves reasonably. Its state changes abruptly after the initial "kick." Then the probabilities experience significant variations during the long half-cycle. In contrast to the previous case $\tau<T_i$ the system is unable to recover at the end of the pulse. The ionization probability does not tend to zero. The ASPA reproduces all these features precisely for $|a_1|^2$. Six negative-energy states are enough. We also see good quantitative agreement for $|a_2|^2$ when $t<5$.

The ASPA with negative-energy states only overestimates $|a_2|^2$ for larger t. It can be corrected partly by accounting for the positive-energy states. The inset of Fig. 10 shows the momentum distribution of the emitted electron. One can see that the correction comes from the states with $n\leq 14$. The populations of higher energy states are small and drop exponentially as $p_n=\sqrt{\epsilon_n}$ increases. Accordingly, our calculations show that the enlargement of $\mathbb{S}_2$ with states $n>14$ does not improve the agreement. We also did calculations with $\mathbb{S}_1$ having only one state with $n=7$ or $n=8$. Interestingly, the agreement was even worse. To explain the discrepancy we recall that the accuracy of our calculations is controlled by parameter α from Eq. (7). It was rather large ($\alpha=0.5$) to let the error develop for sufficiently large time intervals.

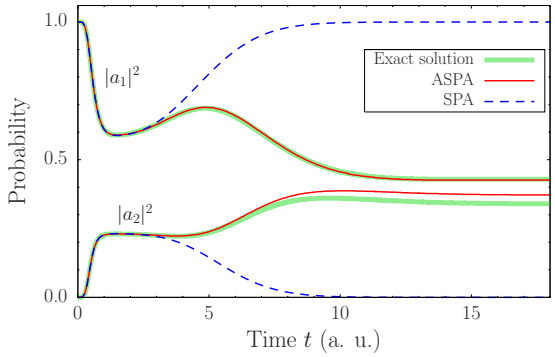

FIG. 11. (Color online) Same as Fig. 10 but with broken blue lines corresponding to $|a_1|^2$ and $|a_2|^2$ calculated with the use of the zero-order SPA.

Finally, we would like to compare the SPA and ASPA results for the case presented in Figs. 10. We see from Fig. 11 that the zero-order SPA is in good agreement with the exact result for sufficiently small t. However, for larger t the condition (1) is violated and no agreement is observed. In the considered case $\Delta p=0$ and, hence, $\hat{S}_0(\infty,-\infty)=\hat{I}$. So, according to the zero-order SPA, the system has to return to the initial state after the pulse action is complete. In contrast the ASPA is valid for all t.

IV. DISCUSSION

The prerequisite of the theory described in Sec. II is the possibility to group the Hilbert space states by their physical properties so that not individual states but the groups of states are accounted for as a whole. This simplifies the consideration significantly as demonstrated. The key point is to find the correct criterion to group the states and corresponding approximation suitable for the conditions of interest.

The strong field approximation [5] can be a logical choice in the case of atoms interacting with very intense fields. It was applied recently in a similar way in Ref. [20]. In that case all excited states of the field-free system are embedded into the continuum and the strong field dominates their dynamics.

We study another extreme specified by condition (7). In general, the ASPA is applicable for any field magnitude and any pulse duration since all states of the Hilbert space are taken into account. This is only subject to computer resources. In addition, the ASPA can be used for description of collision processes in the framework of the impact parameter approximation.

To apply the ASPA fully one has to take properly into consideration the system continuum. Our work reveals that the SPA resolves this problem only partly, for the $\mathbb{S}_1$ continuum only. In the previous section we considered numerical examples where the maximum electron momentum variation due to the field is relatively small and so is the effect of

the S_2 continuum states. The good agreement between the reference and ASPA results testifies that the contributions of S_1 states are accurately encoded in Eq. (20). One could anticipate that the S_2 continuum is of greater importance for stronger fields.

V. SUMMARY

An approach has been introduced to analyze how a pulsed perturbation of arbitrary form affects a quantum system. For some system states this perturbation is sufficiently short so that their contributions in the total wave function are taken into account with the sudden-perturbation approach. The other states are accounted for exactly. The amplitudes of these states can be found from the closed set of their integral equations. Upon solution the whole wave function can be reconstructed. The reported approach has been tested for numerically solvable one-dimensional atomic model. Its application to realistic problems (3D atom interacting with one and two ultrashort pulses) is currently being implemented.

ACKNOWLEDGMENT

One of us (A.L.) would like to thank Genadij Yudin for a number of stimulating discussions.

[1] K. Burnett, V. C. Reed, and P. L. Knight, J. Phys. B **26**, 561 (1993).
[2] A. B. Voitkiv, Phys. Rep. **392**, 191 (2004).
[3] D. Bauer and P. Koval, Comput. Phys. Commun. **174**, 396 (2006).
[4] L. D. Landau and E. M. Lifshitz, *Quantum Mechanics: Non-Relatavistic Theory*, Vol. 3 of Course of Theoretical Physics, 3rd ed. (Pergamon Press, Oxford, 1977).
[5] D. B. Milosevic, G. G. Paulus, D. Bauer, and W. Becker, J. Phys. B **39**, R203 (2006).
[6] A. M. Dykhne and G. L. Yudin, Sov. Phys. Usp. **21**, 549 (1978).
[7] M. T. Frey, F. B. Dunning, C. O. Reinhold, S. Yoshida, and J. Burgdörfer, Phys. Rev. A **59**, 1434 (1999).
[8] M. Klews and W. Schweizer, Phys. Rev. A **64**, 053403 (2001).
[9] B. E. Tannian, C. L. Stokely, F. B. Dunning, C. O. Reinhold, S. Yoshida, and J. Burgdörfer, Phys. Rev. A **62**, 043402 (2000).
[10] E. Persson, S. Yoshida, X.-M. Tong, C. O. Reinhold, and J. Burgdörer, Phys. Rev. A **66**, 043407 (2002).
[11] O. Smirnova, M. Spanner, and M. Ivanov, J. Mod. Opt. **54**, 1019 (2007).
[12] J. Javanainen, J. H. Eberly, and Q. Su, Phys. Rev. A **38**, 3430 (1988).
[13] U. Schwengelbeck and F. H. M. Faisal, Phys. Rev. A **50**, 632 (1994).
[14] M. L. Pons, R. Taïeb, and A. Maquet, Phys. Rev. A **54**, 3634 (1996).
[15] O. Smirnova, S. Patchkovskii, and M. Spanner, Phys. Rev. Lett. **98**, 123001 (2007).
[16] A. M. Dykhne and G. L. Yudin, *Sudden Perturbations and Quantum Evolution* (Uspekhi Fiz. Nauk Publishing House, Moscow, 1996) (in Russian).
[17] I. Bray and A. T. Stelbovics, Phys. Rev. A **46**, 6995 (1992).
[18] A. Bugacov, B. Piraux, M. Pont, and R. Shakeshaft, Phys. Rev. A **51**, 4877 (1995).
[19] A. Wetzels, A. Gurtler, L. D. Noordam, F. Robicheaux, C. Dinu, H. G. Muller, M. J. J. Vrakking, and W. J. van der Zande, Phys. Rev. Lett. **89**, 273003 (2002).
[20] O. Smirnova, M. Spanner, and M. Ivanov, J. Phys. B **39**, S307 (2006).